

A Tetrameric Model of the Dihydrolipoamide Dehydrogenase Component of the Pyruvate Dehydrogenase Complex: Construction and Evaluation by Molecular Modeling Techniques

Günter Raddatz*, and Hans Bisswanger

Physiologisch-Chemisches Institut Universität Tübingen, Hoppe-Seyler-Str. 4, D-72076 Tübingen, Germany;
Tel: +49-7071-297-4180; Fax: +49-7071-29-3360 (guenter.raddatz@uni-tuebingen.de)

Received: 18 August 1997 / Accepted: 7 October 1997 / Published: 24 October 1997

Abstract

On the basis of the homodimeric X-ray structure of dihydrolipoamide dehydrogenase from *Azotobacter vinelandii* we demonstrate by protein modeling techniques that two dimeric units of this enzyme can associate to a tetrameric structure with intense contacts between the building blocks. Complementary structures of the respective other unit in the tetramer contribute to the active sites. The coenzyme FAD becomes shielded from the environment, thus its binding is stabilized. By energy minimization techniques binding energies and RMS-values were computed and the contact areas between the building blocks were determined to quantify the interaction. In the cell tetramerization of dihydrolipoamide dehydrogenase will be realized upon its incorporation as an enzyme component into the pyruvate dehydrogenase multienzyme complex and will have consequences for the structure and subunit stoichiometry of the complex. Especially, the multiplicity of the three enzyme components, i.e. pyruvate dehydrogenase, dihydrolipoamide acetyltransferase and dihydrolipoamide dehydrogenase in the enzyme complex must be 24:24:24 instead of 24:24:12 assumed so far.

Keywords: Subunit-subunit interaction, Dihydrolipoamide dehydrogenase, Multienzyme complex, Protein modeling, Force field calculations.

Introduction

The 3-D structure of the enzyme dihydrolipoamide dehydrogenase has been determined from *Azotobacter vinelandii* [1, 2], *Pseudomonas putida* [3] and *Pseudomonas fluorescens* [4] by X-ray crystallography. Whereas in the free form the enzyme controls the redox equilibrium between dihydrolipoic acid and lipoic acid, it further acts as the E3-component of the alpha-oxoacid dehydrogenase multienzyme complexes, like the pyruvate dehydrogenase complex. Here it has the

function to reoxidize the flexible lipoyllysine arm coupled to the dihydrolipoamide acetyltransferase component E2 [5]. The E2 component forms the core of the multienzyme complex, to which both the pyruvate dehydrogenase (E1) and the dihydrolipoamide dehydrogenase (E3) components bind. The pyruvate dehydrogenase complex from Gram-negative bacteria like *Escherichia coli* possesses 24 identical subunits both of the E1 and the E2 components, while the multiplicity with respect to the E3 component is not completely clear. From quantitative determination of coenzyme FAD bound to the E3 component [6] and from the relative protein content of

* To whom correspondence should be addressed

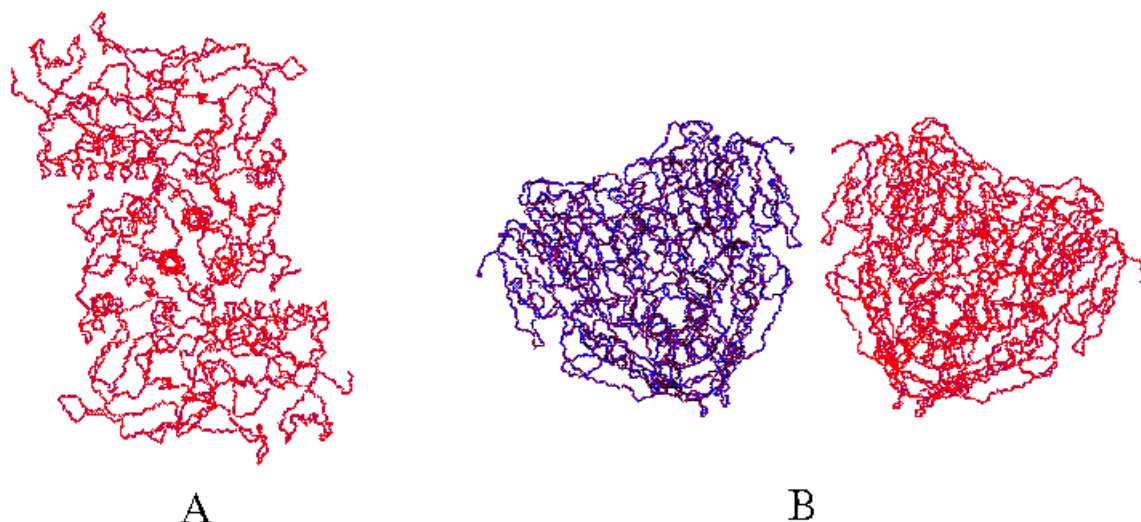


Figure 1. Two different projections of the dihydrolipoamide dehydrogenase dimer. Left) Projection in the direction of the twofold axis. Right) Side-view of two dimers, getting into contact at the 8 nm long side. The twofold axis of the two dimers deviates from the perpendicular fourfold axis of the inner E2-core, because they are turned by the same angle into opposite directions.

the components [7] a multiplicity of 12 subunits has been postulated [8], while experiments from other groups support a stoichiometry of 24:24:24 [9, 10, 11]. Although the subunit stoichiometry of 24:24:12 became widely accepted [5, 12] some theoretical arguments are against this. The 24 E2 subunits contribute 24 identical peripheral subunit binding domains [13, 14, 15, 16] to stabilize the binding of the E1 and the E3-component to the core complex. It is assumed, that each such domain is able to anchor one E1 dimer [5], which leads to the occupancy of 12 of the 24 peripheral subunit-binding domains, leaving 12 domains unbound. As recently shown by Mande et al. [17] one dimer of the E3 is bound by one subunit-binding domain. Consequently 12 E3-dimers should be attached to the complete octahedral PDC complex. Indeed it is not obvious, which reasons prevent the smallest subunits of the enzyme complex from binding to its free binding sites, especially as there exists a surplus of unbound dihydrolipoamide dehydrogenase in the cell [18].

Electron microscopy [19] as well as the recently resolved X-ray structure of a truncated E2 component [12, 20] revealed that in the pyruvate dehydrogenase complex from Gram-negative bacteria 24 E2 subunits aggregate to a regular cube with a hole in its middle. The edges of the cube are occupied by 24 E1 subunits and the six faces by the E3 component. Assuming a multiplicity of 12, one dihydrolipoamide dehydrogenase dimer will bind per face, whereas a 24-fold multiplicity requires the binding of a tetramer.

The X-ray structure of dimeric dihydrolipoamide dehydrogenase from *Azotobacter vinelandii* allows to decide, whether the formation of functional tetrameric E3 structures within the multienzyme complex structure may be possible in principal. We demonstrate with protein modeling techniques and force field calculations that two dimeric dihydrolipoamide dehydrogenase molecules are able to aggregate to compact tetrameric units. These are superior to the dimeric structure in complete shielding of the FAD coenzyme binding fold from the environment and a completion of the catalytic center by parts of the other dimeric unit.

Modeling Methods

All modeling procedures were performed applying the program SYBYL 6.3 [21] on a Silicon Graphics IRIS Indy workstation. The conjugate gradient geometry optimization was realized with the program AMBER 4.0 [22] running on a CONVEX C220. The Kollman all atom force field was used. As starting coordinates the reported X-ray structure of dihydrolipoamide dehydrogenase from *Azotobacter vinelandii* (entry: 3LAD) [2] from PDB [23] was chosen. Preference was given to this structure over the respective structures from *Pseudomonas putida* (entry 1LVL, [3]) and *Pseudomonas fluorescens* (1LPF, [4]) since it is typical for the octahedral Gram-negative pyruvate dehydrogenase complex. The sidechains of the residues Lys36, Glu39 and Lys41, which were invisible in the crystal structure, were introduced according to canonical structures. In order to resolve steric conflicts created by the contact between sidechains of the two dimeric structures alternative rotamers were tested at the relevant positions until most van der Waals contacts were eliminated. The constructed model was solvated in a shell of TIP3P-water and geometry optimized by 5000 steps conjugate gradient energy minimization, setting the non-bonded cutoff to

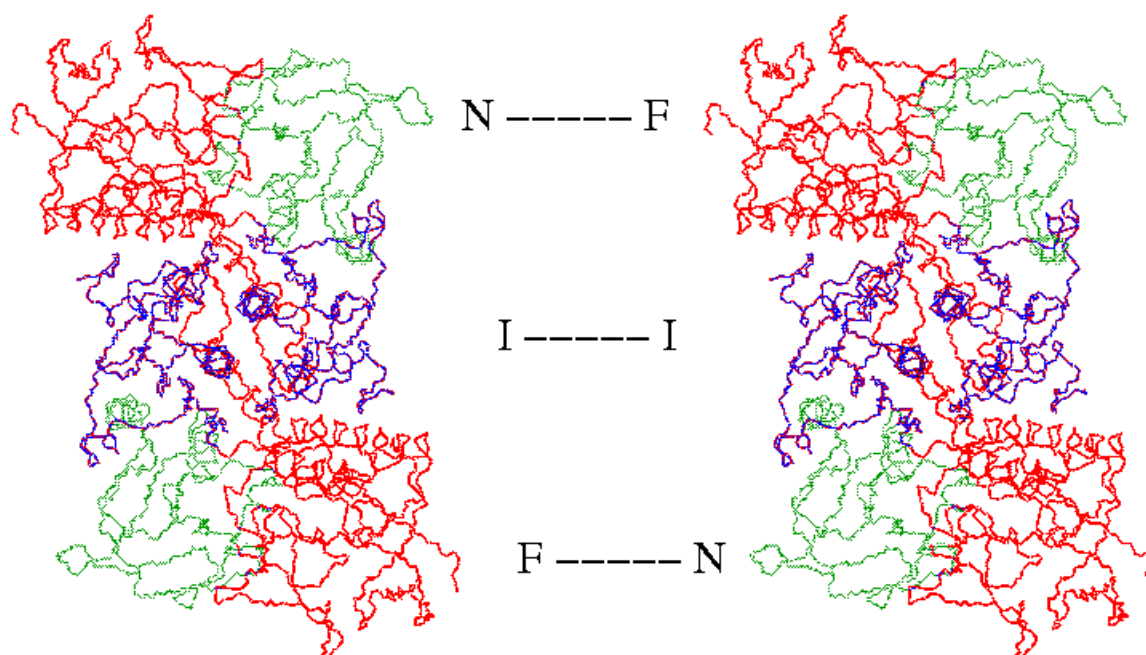


Figure 2. Orientation of the alignment of two dihydrolipoamide dehydrogenase dimers. The contacts between the NAD (*N*) and the FAD domains (*F*), and the interface domains (*I*) are indicated.

7.0 Å. The partial charges for the coenzyme FAD were computed by a semiempirical PM3-calculation with the program MOPAC 6.0 [25]. Solvent accessible surfaces were computed using the program DSSP [26]. The constructed model was subjected to the programs WHAT_CHECK, PROCHECK and SURVOL, available at the EMBL Heidelberg. SURVOL calculates for each atom in a given structure the atomic volume and compares these volumes with a pre-computed average for each atom type. From this a structural average “absolute Z-value” is calculated. This value is expected to be around 0.82 for an average structure. Values are considered poor if they are larger than 1.0 and bad, if they are higher than 1.2. The aim of PROCHECK is to assess the overall stereochemical quality of a given protein structure, as compared with well-refined structures at the same resolution. PROCHECK produces a value called “overall average G-factor” to estimate the quality of the whole structure. This value is considered poor if it is less than -0.5 and bad, if it is less than -1.0. WHAT_CHECK checks a variety of properties of a protein structure, like e.g. incorrect bond lengths, bad van der Waals contacts and buried unsatisfied h-bond donors and acceptors. Although during the last years a couple of docking-programs have become available (see [35] for a review of the different algorithms applied) the principal construction of the tetrameric structure was done without these tools and relies on the arguments outlined in the following section. This was

preferred due to the drastic reduction of conformational space of the tetrameric model which is enabled by the described arguments. Furthermore, the local energy-barriers, that obviously have to be overcome by the dimeric structures to form the tetramer are known to be problematic for automated docking-programs [35].

Results

Construction of the tetrameric model

The first step for the construction of the tetrameric model of dihydrolipoamide dehydrogenase consists in principal considerations concerning the orientation of both dimeric units relative to one another. Special attention has to be paid to a) the inside-outside orientation of the dimeric units with respect to the complete pyruvate dehydrogenase complex, b) the principal contactplane of the dimeric units and c) considerations about possible rotations of the dimeric units in the constructed tetramer.

The crystallization experiments of Mattevi et al. [12,20] showed that the faces of the E2 cube of the pyruvate dehydrogenase complex obey a fourfold symmetry, the symmetry-axis directing to the center of mass of the complex structure. Therefore, the postulated tetrameric structure which interacts with this face must be determined also by this fourfold symmetry. This is realized by aligning the twofold axis of the dimeric units to the fourfold axis of the pyruvate dehydrogenase complex inner core. This assumption, which was already stated by Mattevi et al. [2], allows two possible orientations of the E3 twofold axis, differing by a rotation of

180 degree around an axis perpendicular to the twofold one and positioning either the upper or the lower region of the E3-dimer onto a face of the inner core. In [2] it was assumed that the lower region is oriented toward the face of the truncated inner cube, because this orientation allows the shortest distance between the centers of gravity of E2 and E3. A further argument supports this assumption. The binding site of the cosubstrate NAD, which is located at the upper site of the E3 subunit, should open to the surrounding medium to enable free access of NAD and removal of NADH. Because this, as well as the arguments given in [2] is valid for both dimeric units, opposite orientations of both dimers are ruled out.

To identify the contact region between both dimeric units, a projection of an E3 dimer onto the plane perpendicular to the twofold axis of symmetry corresponding to one face of the inner cube reveals a striking feature. In this projection the dimer shows a nearly perfect 4×8 nm rectangular structure (Fig. 1A). Thus, alignment of two dimers with both their long sides yields an approximately 8×8 nm regular square structure of a tetramer fitting excellently to the cube face.

It has to be mentioned, that the exact alignment of the twofold axis of E3 to the fourfold axis of the inner core is really valid only for the complete tetrameric structure. So the twofold axis of the dimeric E3 units can deviate from this alignment, as long as the alignment of twofold axis of the tetramer remains preserved. This allows an orientation of the two dimers to one another as shown in Fig 1B.

From the above considerations the domain-domain contacts between two E3-dimers can be concluded. The NAD domain (N) of the subunit of one dimer faces the FAD domain (F) of the corresponding subunit of the other dimer (Fig. 2). These two contact areas are separated by the interface domains (I), which get into plane contact with one another.

Considering these arguments the principal architecture of the tetrameric structure is predetermined. The procedure of concrete model building started with the examination of the detailed secondary structure elements in the contact area of the two components. Stringent criteria are: i) distortions of the active site had to be avoided, ii) the entrance of NAD to its binding site must remain open. The model construction concentrated more on the elaboration of the F-N contacts between the NAD and FAD domains with their highly structured surfaces, than on the I-I contacts of the plane interface domains. Since F-N contact areas exist at both sites of the alignment (Fig. 2) the enclosed I-I contacts were definitely fixed as a result of the modeled F-N interaction. Consequently, the appearance of a reasonable contact between the secondary structure elements of the interface domains can be considered as a first test for the validity of the model.

The most remarkable structural feature of the F-N contact area is represented by the two peripheral helices Val87:Gly113 (helix 1.3 according to the classification given in [2]) and Asp220:Gln234 (helix 2.6) belonging to the FAD-domain and the NAD-domain, respectively (Fig. 3A). Since

both helices assume equivalent positions at the 8 nm alignment site between the two dimers they must get into direct contact with one another. It is very striking, that both these peripheral helices are separated from their respective domains by empty channels, which are exactly suited both in size and topology to bury the complementary helix inside the other domain (Fig. 3B). This causes a very intense contact of the two components. Obviously this tight interaction determines the relative orientation of both dimeric units to one another. The nearly parallel arrangement of the helices 1.3 (Val87:Gly113) and 2.6 (Asp220:Gln234) dictates the deviation of the individual dimers from the twofold axis. Because of the symmetric helix-helix contact of the second N-F-interaction occurring in the dimer-dimer model there remains only minor freedom for interactive docking of the dimeric building blocks. Consequently, the interactions of all other areas of the dimeric units are predetermined and the reasonableness of these interactions, which fit without essential steric or electrostatic hindrances strongly supports this approach.

Structural and energetic features of the tetrameric arrangement

The projection of the tetrameric arrangement onto the plane perpendicular to its twofold axis (Fig. 4a) demonstrates the tight interaction of the dimeric units and the nearly ideal square shape of the tetramer, which fits well to the face of the cubic core of the pyruvate dehydrogenase complex. The two interface domains fit plane to one another and show nearly perfect hydrophobic interactions without any steric conflicts. The solvent accessible surface of the tetramer, evaluated by the program DSSP [26] is 56088 \AA^2 . After tetramerization 8051 \AA^2 per dimer became buried, corresponding to a loss of 22.2 % of the solvent accessible surface of the free dimeric structure. The monomer area contributing the interface and the FAD domains to the dimer-dimer contact lost 5201 \AA^2 solvent accessible surface, while 2850 \AA^2 of the surface of the monomer area contributing the NAD domain became buried. In comparison to the remarkably high value for the dimer-dimer interaction only 12.6 % and 16.0 % of solvent accessible surface become lost by monomer-monomer interactions for dihydroliipoamide dehydrogenase of *Azotobacter vinelandii* and *Pseudomonas fluorescens*, respectively [2, 3].

In order to evaluate the energetics of the dimer-dimer interaction the energy minimization method as described in METHODS has been applied. Due to limited computational resources the model was split into two parts, one consisting of the two contacting interface domains and the other of two monomers with interacting FAD- resp. NAD-domains, but without interface domains. This procedure is justified by the sharp partition of these two contact areas.

The I-I part of the model relaxed to an AMBER all atom energy of -16986.1 kcal/mol and showed a RMS-difference (RMSD) of 0.69 resp. 0.72 Å for the two interface domains from the C-alpha atoms of the crystal structure. Similar en-

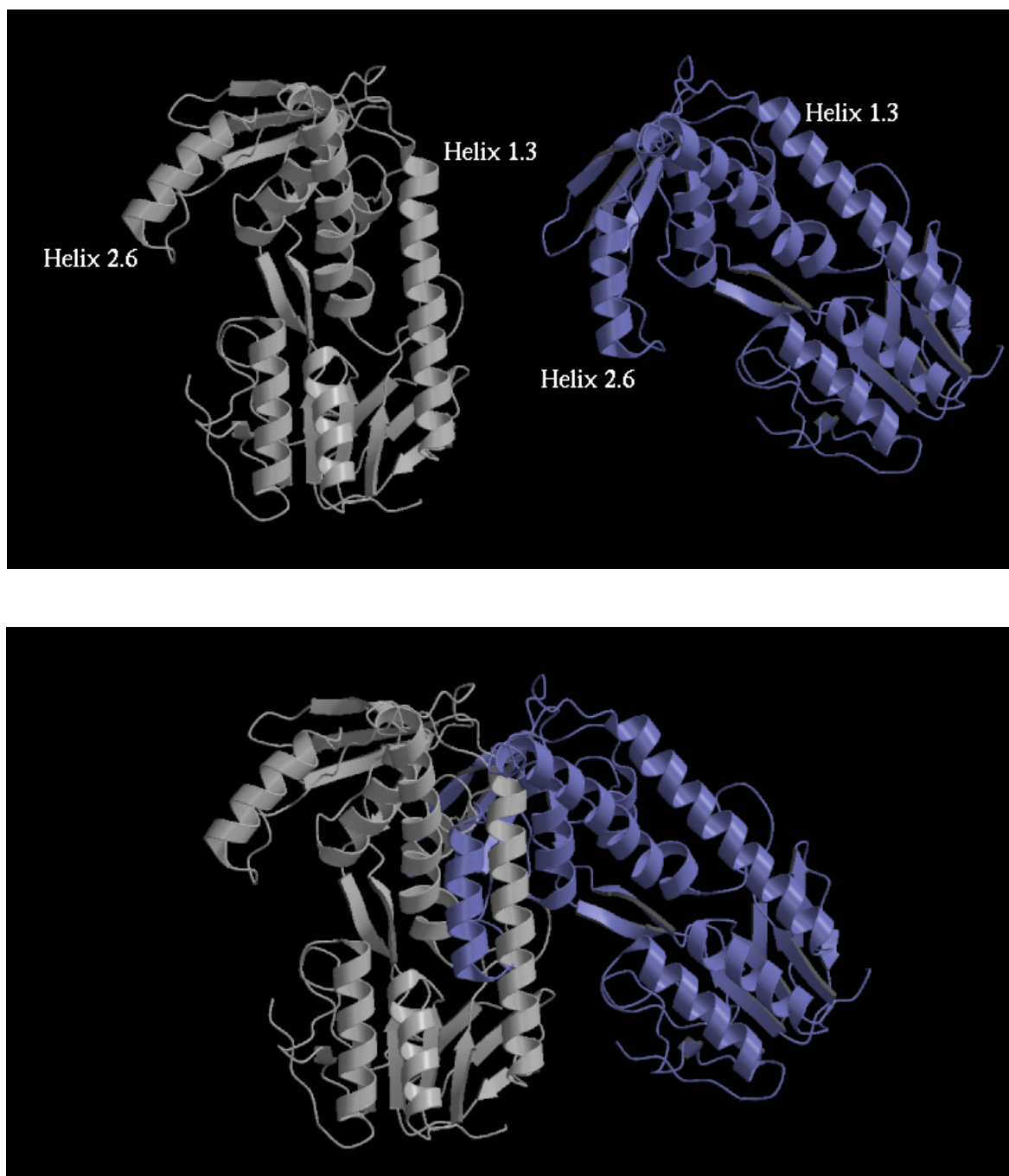


Figure 3. Aligment of the peripheral helix 1.3 (Val87: Gly113) from the FAD domain of one dimeric unit (left, pale) with the helix 2.6 (Asp220:Gln234) of the NAD domain from the other dimeric unit (right, dark). Top: Separate presentation. Bottom: Aggregated form. The units are reduced to one monomer without interface domain. The picture was produced with the programs Molscript [33] and Raster3D [34].

ergy minimization of a single, free interface domain resulted in an RMSD of 0.61 Å. The minimized model showed an energy of interaction between the two interface domains of -164.4 kcal/mol, nearly equally distributed to the non-bonded (-76.3 kcal/mol) and the electrostatic/H-bond (-88.1 kcal/mol) part. The evaluation with the AMBER Anal-modul revealed 22 H-bonds between the two domains. The check of the quality of the I-I model, using the program SURVOL, resulted in a volume score of 0.9 concerning the backbone and 0.8 concerning the sidechain atoms. The average value for the whole structure was 0.9, which is near to the optimal value of 0.82.

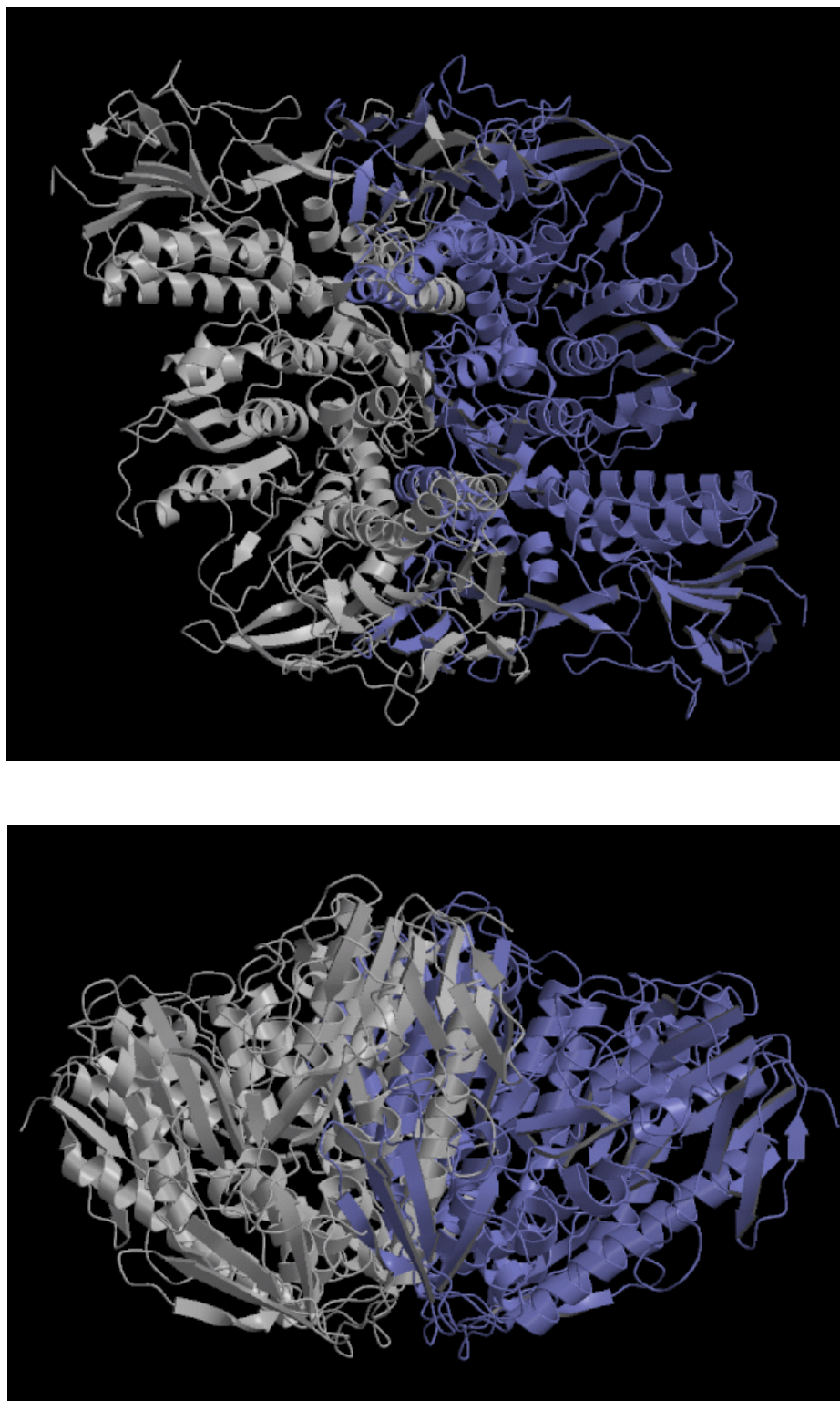


Figure 4. Tetrameric arrangement of dihydrolipoamide dehydrogenase. Dimer 1 is colored white, dimer 2 cyan. Top: View-axis aligned with the twofold axis of the tetramer. Bottom: Side-view. The picture was produced with the programs Molscript [33] and Raster3D [34].

The overall average G factor, computed with PROCHECK, amounted to -0.20. All these values are in the range, which indicates an acceptable structure. The investigation of the model with WHAT_CHECK revealed no essential problems caused by the modeled subunit-subunit contact. A few unsatisfied h-bond donors resp. acceptors were found in the con-

Table 1. Kollman all atom force field energies of the I-I part and the F-N part of the model solvated in a shell of TIP3P-water after 5000 steps conjugate gradient geometry optimization (kcal/mol).

	F-N Model	I-I Model
Total Energy	-46299.0	-16986.1
Bond	692.0	294.3
Angle	1167.7	459.6
Torsion	1205.0	369.7
VdWaals	-1703.3	-467.0
Electrostatics	-46799.0	-17331.9
H-Bond	-861.7	-310.8

tact area, which probably could be compensated by embedded water molecules.

The F-N part of the model relaxed to a force field energy of -46299.0 kcal/mol. The RMSD of the 350 C-alpha atoms to the X-ray structure is 1.01 Å for the monomer contributing the NAD domain and 1.42 Å for the monomer contributing the FAD domain. The RMSD for a single, free such structure after the minimization procedure yielded a value of 0.80 Å. The RMSD caused by the contact of the FAD and NAD domains, which is higher than with the I-I-part, reflects the more complex nature of this interaction, which may cause some local distortions of the backbone. The interaction energy of the NAD and FAD domains of the two monomers was -483.6 kcal/mol, dominated by the electrostatic part. This is also reflected by the high number of 210 H-bonds formed between the NAD and the FAD domains. For the tetramer the twofold amount of H-bonds must be considered because of the twofold appearance of the NAD and FAD contacts. The check of the quality of the F-N model, using the program SURVOL, resulted in a volume score of 0.9 concerning the backbone and 1.0 concerning the sidechain atoms. The average value for the whole structure was 0.9. The overall average G factor, computed with PROCHECK, amounted to -0.36. As with the I-I-model, all values are in the range, which indicates an acceptable structure. The investigation of the F-N model with WHAT_CHECK indicated, as with the I-I model, no essential problems caused by the modeled subunit-subunit contact. Again a few unsatisfied h-bond donors resp. acceptors were found in the contact area, which probably could be compensated by embedded water molecules.

Interaction of the NAD and FAD domains

Since the peripheral helix 1.3 (Val87:Gly113) in the FAD domain of dimer 1 is close to the active site, the helix 2.6 (Asp220:Gln234) contributed from dimer 2 gets into direct vicinity of the catalytic center and distortions of the sensible

active site structure as well as impediment of catalytic residues must be suspected. It turns out, however, that helix 2.6 of dimer 2 as well as the adjacent residues carefully surround the segment CLNVGC containing the catalytically active Cys48-Cys53 disulfide group of dimer 1 (Fig. 5). This embedding may contribute to the stabilization of the active site or it may modulate the affinity to the ligands by inter-dimer movements in the operating pyruvate dehydrogenase complex.

The mutual interaction of both helical segments gives a further possibility to prove the reliability of the model. To achieve this type of interaction the two helices must find an access into the complementary structure. It is again the distinct structure of the helix 2.6 of dimer 2 which allows it to switch below the helix 1.3 of dimer 1 into its final position. This can be seen from Fig. 5, where the cyan coloured helix of the second dimeric unit intercalates between the active site and the white coloured helix of the first unit. It must be emphasized, that this arrangement would not be possible, if the parts of the polypeptide chain continuing the helix 2.6 at both its ends would point into opposite directions.

Contacts are formed also between FAD bound to the FAD domain and three peripheral loop structures of the NAD domain from the other dimeric unit (Fig. 6). These are the loops Ala211:Val219, which connects the beta-strand C2 with the

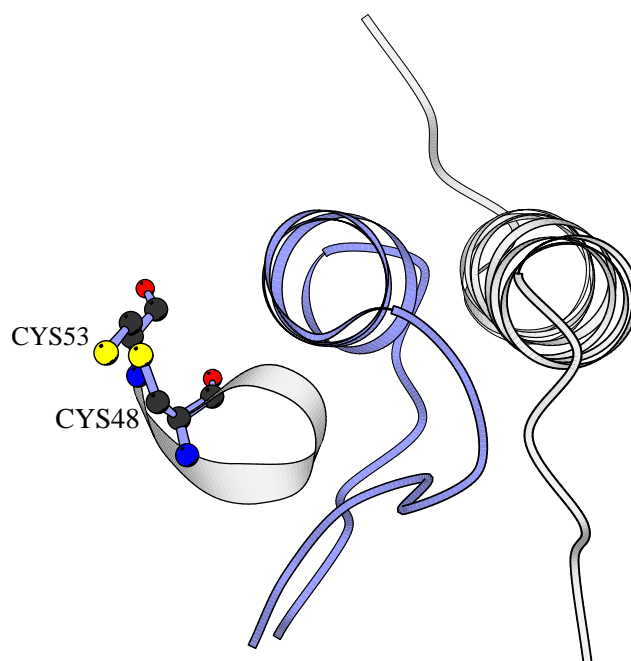


Figure 5. The 'overlapping' helices 1.3 of dimer 1 (white), 2.6 of dimer 2 (cyan) and part of the active site of dimer 1 containing the redox active thiol groups (yellow) of Cys48 and Cys53.

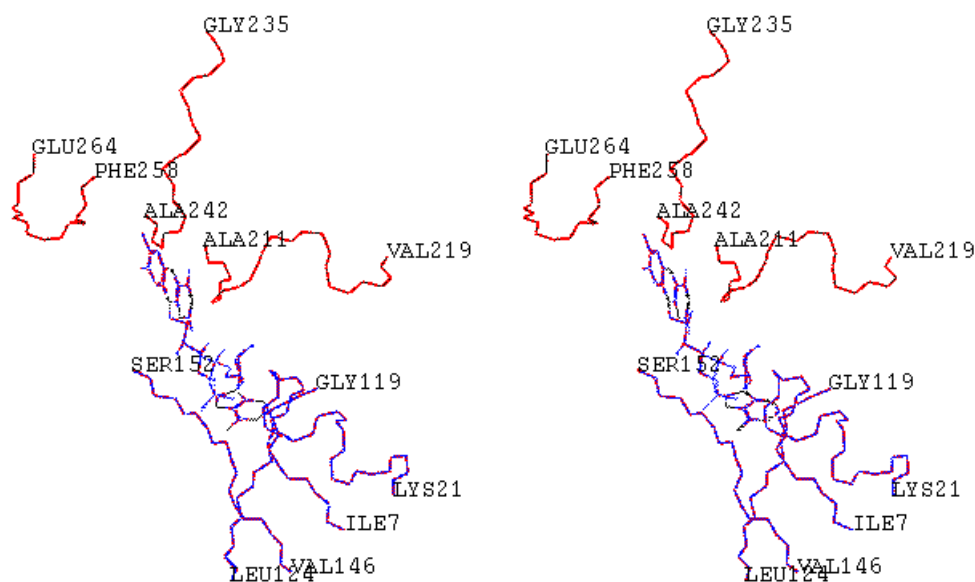


Figure 6. Stereo view of the FAD binding region to demonstrate the shielding of solvent exposed parts by loops of the additional dimeric unit. Residues belonging to the first dimeric unit are coloured blue, those of the additional unit red. The first and the last amino acid of each segment are labelled.

helix 2.6, Gly235:Ala242 which connects the helix 2.6 with the beta-strand D1 and Phe258:Glu264, which connects the beta-strands D2 and D3. The interaction takes place mainly with the adenosine and the diphosphate part of FAD, which remains partially solvent accessible in the free dihydrolipoamide dehydrogenase structure. The contact causes a significant loss of the remaining solvent accessible surface and leads to interaction energies of -26.2 kcal/mol in the geometry optimized model. In [2] the interaction of FAD with surrounding amino acids of free dihydrolipoamide dehydrogenase was analyzed and the uncompensated negative charge of the diphosphate part discussed. In the tetrameric arrangement this charge can be compensated by the positive charge of Lys214, which is positioned in the first of the three loops and whose C-alpha is 6.0 Å distant from the adenosine phosphate. This shielding of the FAD binding pocket in the tetrameric arrangement is conform with the observation that this coenzyme is bound extremely tight in the pyruvate dehydrogenase complex [27] and it guarantees the presence of the coenzyme during the catalytic sequence of the multienzyme complex.

Interaction of the interface domains

In contrast to the F-N interactions the interface domains fit plane together (Fig. 7A). The two anti-parallel beta-strands

Val381:Ala387 and Ala399:Ile405, as well as the carboxyterminal residues Ile469, His470, Val471 and Ala472 of the both interface domains contribute to these interactions (Fig. 7B). It is remarkable that in the free dimeric structure the solvent exposed residues Val381, Val383, Pro385, Ala387, Ala399, Phe401 and Ile405 of the two beta-strands are strongly hydrophobic, with the only exception of Lys403. This unusual exposition of hydrophobic residues on the protein surface is completely lost in the tetrameric structure. The energy gain due to an entropy increase may be a significant driving force for the tetramerization of the E3 subunits in the pyruvate dehydrogenase complex. Lys403 forms H-bonds with the oxygens from the backbone of the carboxyterminal residues Ile469 and His470 of the opposite interface domain, which are unsaturated in the free dimer. This stabilizes the residue His470, which is supposed to be involved in the binding and the catalytic reaction of the substrate [2].

Discussion

The tetrameric model of two dihydrolipoamide dehydrogenase dimers is based on symmetry considerations dictated by the fourfold axis of the E2 core and it fulfills the expectations and requirements in a convincing manner. The model is supported, however, not only by structural, but also by functional features. As is observed already with numerous oligomeric enzymes, both units contribute elements to complete and support functions of the respective other unit. It is well known that FAD, although not covalently bound, cannot easily be dissociated from the pyruvate dehydrogenase complex [27]. Solely from the structure of the dihydrolipoamide dehydrogenase dimer this extremely tight binding cannot be

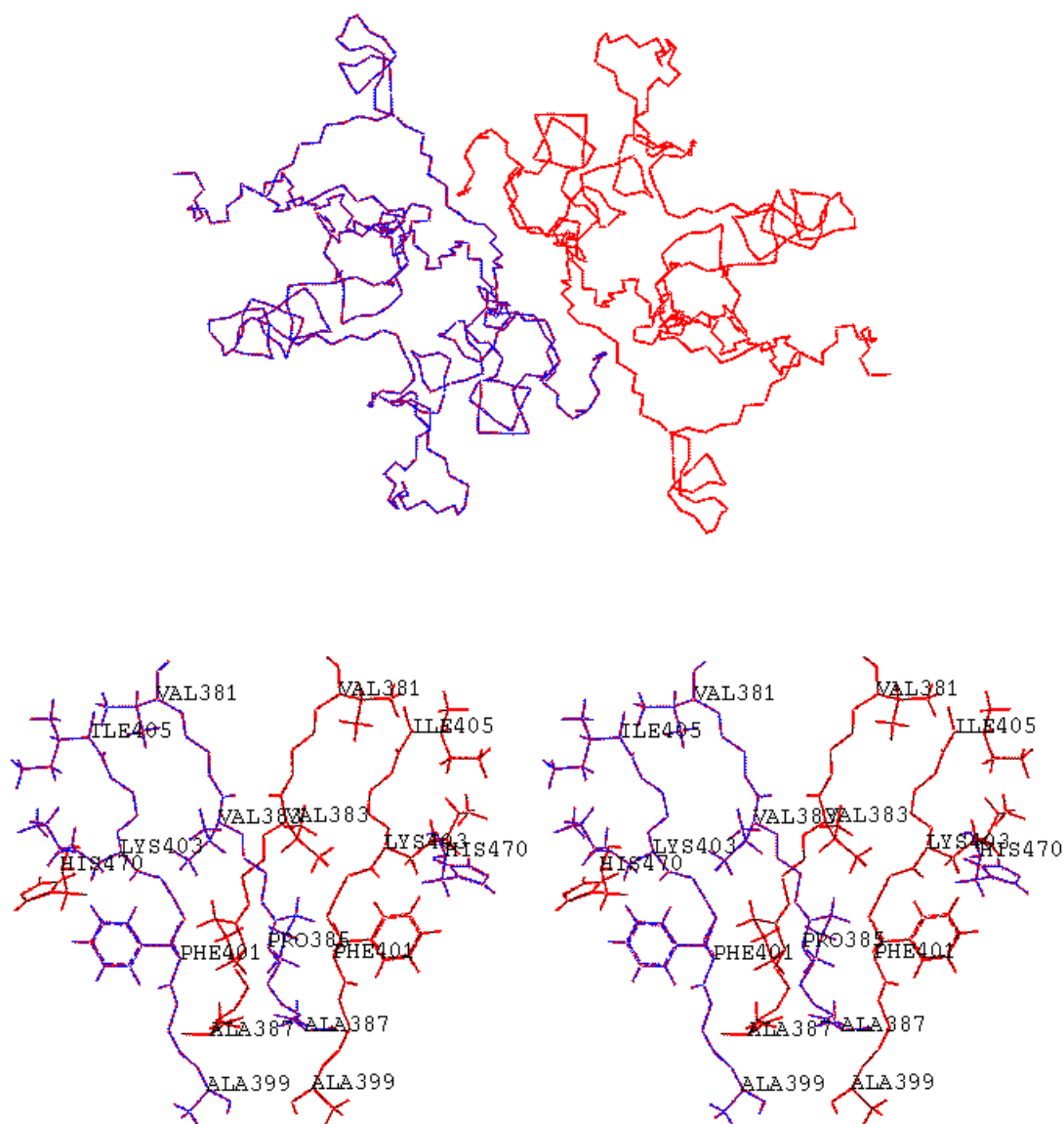


Figure 7. View of the interaction between the two interface domains. A) The complete interface domains. View axis aligned with the twofold axis of the tetramer. B) Detailed representation of the interaction between the beta-strands Val381:Ala387 and Ala399:Ile405, and the C-terminal amino acids of the both interface domains. Residues belonging to the first dimeric unit are coloured blue, those of the additional unit red.

understood, but the shielding of solvent accessible parts of the coenzyme by the NAD domain of the opposite dimer in the tetrameric arrangement gives a clue to understand this feature. Another example for the cooperation of both dimeric units in one function is the interaction of the helix 2.6 with the catalytic site of the other unit.

The postulated model has severe consequences for architecture and stoichiometry of the Gram-negative pyruvate dehydrogenase complex. A ratio of 24:24:24 for the subunits of the three enzyme components must be assumed, though lower amounts of E3 subunits were reported [6]. There lack, however, convincing arguments for what should prevent the E3 subunits from occupying their preexisting binding domains at the E2 core. The E3 subunits are the smallest ones of the enzyme complex and there is no reason to assume sterical hindrance for a tetramer to bind to the square cube face. Sterical hindrance may occur with the adjacent E1 subunits. The contact between the E1 and E3 subunits is determined by the topology of the E1 and E3 binding sites at the E2 core and the relative orientation of the respective subunits bound. Due to symmetry this is identical for the both first and the second E3 dimer bound. The intense fit of both dimers in the

tetrameric arrangement rules out a half-of-the-sites reactivity [28], i.e. impeding of the binding of a second dimer by the already bound first dimer.

With the pyruvate dehydrogenase complexes from various sources it has been observed that binding of the E3 component to the core is relatively weak and part of the subunits were lost during purification even when the complexes are carefully prepared [29, 30]. This fact may be responsible for an underestimation of the FAD content after its extraction from the enzyme complex [6].

The fact that tetramers are not seen in the resolved X-ray structures of dihydrolipoamide dehydrogenase apparently argues against the postulated tetrameric arrangement. However, it first must be considered, that unlike enzymes aggregating in tetrahedral structures like lactate dehydrogenase (LDH) and glyceraldehyde-3-phosphate dehydrogenase (GAPDH), heterologous aggregations as discussed here will not lead to stable tetramers but to polymeric structures, since aggregation proceeds at either of their long sides. Such structures are extremely disadvantageous for the cell and so it should be expected that the free dimer has no tendency for aggregation. The tetrameric structure should only be formed at the multienzyme complex, which stabilizes this structure and prevents it from further polymerization. The type of interactions between the two dimers in the tetrameric structure answers the question why spontaneous aggregation of dimers does not occur. The formation of the stable F-N contacts requires the penetration of the helix 2.6 of the one dimeric unit into a channel behind helix 1.3 of the other unit. Although the access to this channel is principally opened it is obvious that an energy barrier must be surmounted, which is too high for the free dimers. Binding to and interaction with the E2 core will bring both dimers into a favourable orientation to one another to achieve the contact and to reduce the energy necessary to overcome the barrier.

The tetrameric arrangement has further consequences for the understanding of the interaction of the E3 component with the flexible lipoyl domain at the E2 component. We were able to identify the penetration site of the lipoyllysine residue of this domain to the catalytic center of dihydrolipoamide dehydrogenase by molecular modeling techniques [31]. With this information it was possible to localize the peripheral binding region of the lipoyl domain. The 3-D structure of this domain from *Bacillus stearothermophilus* has recently been resolved by NMR-spectroscopy [32] and revealed a bulky structure consisting of 80 amino acids arranged in seven beta-strands. However, there still does not exist any knowledge about the interaction of this domain with the pyruvate dehydrogenase complex components on the molecular level. The tetrameric model provides now this information for the E3 component, since both the location of the lipoyllysine penetration site and the complete structural environment of this site in tetrameric dihydrolipoamide dehydrogenase allow the development of a structural model for the binding of the lipoyl domain.

Conclusion

In the presented study we demonstrate on the basis of the X-ray structure of homodimeric dihydrolipoamide dehydrogenase from *Azotobacter vinelandii* by protein modeling techniques, that two dimeric units of this enzyme can associate to a tetrameric structure with intense contacts between the building blocks. The tetrameric arrangement of two dihydrolipoamide dehydrogenase dimers in the pyruvate dehydrogenase complex is concise, other orientations appear grossly improbable. The constructed tetrameric structure of the dihydrolipoamide dehydrogenase dimers from *Azotobacter vinelandii* results in a regular square aggregate without serious steric conflicts between the two dimeric units. This is reflected by the low RMSD-values obtained by the minimization procedure for the I-I contacts and the acceptable values for the F-N contacts. The new contacts formed are surprisingly intense as is demonstrated by the considerably high interaction energies and the loss of large amounts of solvent accessible surface, which exceeds even the monomer-monomer contact in the original dimer. The constructed model has important consequences for the subunit stoichiometry of the whole multienzyme complex. The multiplicity of the three enzyme components, i.e. pyruvate dehydrogenase, dihydrolipoamide acetyltransferase and dihydrolipoamide dehydrogenase in the enzyme complex must be 24:24:24 instead of 24:24:12 assumed so far.

Supplementary material: two partial models (I-I contact, F-N contact) of tetrameric E3 as PDB-files

References

1. Schierbeek, A.J.; Swarte, M.B.A.; Dijkstra, B.W.; Vriend, G.; Read, R.J.; Drenth, J.; Hol, W.G.J. *J. Mol. Biol.* **1989**, *206*, 365-379.
2. Mattevi, A.; Schierbeek, A.J.; Hol, W.G.J. *J. Mol. Biol.* **1991**, *220*, 975-94.
3. Mattevi, A.; Obmolova, G.; Sokatch, J.R.; Betzel, C.; Hol, W.G.J. *Proteins* **1992**, *13*, 336-351.
4. Mattevi, A.; Obmolova, G.; Kalk, K.H.; van Berkel, W.J.; Hol, W.G.J. *J. Mol. Biol.* **1993**, *230*, 1200-1215.
5. Perham, R.N. *Biochemistry* **1991**, *30*, 8501-8512.
6. Eley, M.H.; Namihara, G.; Hamilton, L.; Munk, P.; Reed, L.J. *Arch. Biochem. Biophys.* **1972**, *152*, 655-659.
7. Angelides, K.J.; Akkiyama, S.K.; Hammes, G.G. *Proc. Natl. Acad. Sci. USA* **1979**, *76*, 3279-3283.
8. Hackert, M.L.; Oliver, R.M.; Reed, L.J. *Proc. Natl. Acad. Sci. USA* **1983**, *80*, 2907-2911.
9. Vogel, O.; Hoehn, B.; Henning, U. *Proc. Natl. Acad. Sci.* **1972**, *69*, 1615-1619.
10. Hale, G.; Perham, R.N. *Biochem. J.* **1979**, *177*, 129-137.

11. Bates, D.L.; Harrison, R.A.; Perham, R.N. *FEBS Lett.* **1975**, *60*, 427-430.
12. Mattevi, A.; Obmolova, G.; Schulze, E.; Kalk, K.H.; Westphal, A.H.; de Kok, A.; Hol, W.G.J. *Science* **1992**, *255*, 1544-1550.
13. Reed, L.J.; Pettit, F.H.; Oliver, R.M. *Proc. Natl. Acad. Sci. USA* **1975**, *76*, 3068-3072.
14. Kalia, Y.N.; Brocklehurst, S.M.; Hipps, D.S.; Appella, E.; Sakaguchi, K.; Perham, R.N. *J. Mol. Biol.* **1993**, *230*, 323-341.
15. Packman, L.C.; Hale, G.; Perham, R.N. *EMBO J.* **1984**, *3*, 1315-1319.
16. Radford, S.; Laue, E.; Perham, R.N.; Martin, S.R.; Appella, E. *J. Biol. Chem.* **1993**, *264*, 767-775.
17. Mande, S.S.; Sarfaty, S.; Allen, M.D.; Perham, R.N.; Hol, W.G.J. *Structure* **1993**, *4*, 277-286.
18. Guest, J.R. *Adv. Neurol.* **1978**, *21*, 219-244.
19. Reed, L.J.; Oliver, R.M. *Brookhaven Symp. Biol.* **1968**, *21*, 397-410.
20. Mattevi, A.; Obmolova, G.; Kalk, K.H.; Westphal, A.H.; de Kok, A.; Hol, W.G.J. *J. Mol. Biol.* **1993**, *230*, 1183-1199.
21. TRIPOS Associates. Molecular Modeling Program 6.0 Tripos Associates: St. Louis, MO, 1994.
22. Pearlman, D.A.; Case, D.A.; Caldwell, J.C.; Siebel, G.L.; Singh, U.C.; Weiner, P.; Kollman, P.A. AMBER 4.0. University of California: San Francisco, 1991.
23. Bernstein, F.C.; Koetzle, T.F.; Williams, G.J.B.; Meyer, E.F. Jr; Brice, M.D.; Rodgers, J.R.; Kennard, O.; Shimanouchi, T.; Tasumi, M. *J. Mol. Biol.* **1977**, *112*, 535-542.
24. Weiner, S.J.; Kollman, P.A.; Nguyen, D.T.; Case, D.A. *J. Comput. Chem.* **1986**, *7*, 230-252.
25. Stewart, J.J.P. MOPAC: A semiempirical molecular orbital program. *J. Comput. Aided Mol. Design* **1990**, *4*, 1-105.
26. Kabsch, W.J.; Sander, C. *Biopolymers* **1983**, *22*, 2577-2637.
27. Koike, M.; Reed, L.J.; Carroll, W.R. *J. Biol. Chem.* **1960**, *235*, 1924-1930.
28. Levitzki, A.; Koshland, D.E. *Curr. Top. Cell Regul.* **1976**, *10*, 1-40.
29. Williams, C.H. *The Enzymes* **1976**, *13*, 89-173.
30. Lehmacher, A.; Bisswanger, H. *Biochem. (Life Sci. Adv.)* **1988**, *7*, 29-33.
31. Raddatz, G.; Bisswanger, H. *Journal of Biotechnology*, in press.
32. Dardel, F.; Davis, A.L.; Laue, E.D.; Perham, R.N. *J. Mol. Biol.* **1993**, *229*, 1037-1048.
33. Kraulis, P.J. *J. Appl. Crystallogr.* **1991**, *24*, 946-950.
34. Merritt, E.A.; Murphy, M.E.P. *Acta Cryst.* **1994**, *D50*, 869-873.
35. Janin, J. *Prog. Biophys. Molec. Biol.* **1995**, *64*, 145-166.